J. Min. Metall. Sect. B-Metall. 61 (3) (2025) 357 - 368

Journal of Mining and Metallurgy, Section B: Metallurgy

THE INFLUENCE OF NICKEL GRADE AND ITS OCCURRENCE STATE ON HIGH PRESSURE ACID LEACHING BEHAVIOR OF LATERITIC NICKEL ORES

Aad Alief Rasyidi Baking [a, *], Lejun Zhou [a], Wei Liu [b]

[a] School of Metallurgy and Environment, Central South University, Changsha, PR China
[b] Research and Development Department of QMB Indonesia, Morowali, Indonesia

(Received 08 March 2025; Accepted 03 December 2025)

Abstract

This research evaluates the effects of nickel grade and occurrence state on the leaching behavior of lateritic nickel ores using high-pressure acid leaching (HPAL) at 250 °C with sulfuric acid. Three ores were selected for the study: Ore 1 (ultra-low-grade limonite, 0.73 wt.% Ni), Ore 2 (limonite, 1.34 wt.% Ni), and Ore 3 (saprolite, 2.00 wt.% Ni). Mineralogical studies (XRD, SEM, and EPMA) were conducted to provide insight into nickel-hosting phases and characteristics of the ore matrix. A higher nickel grade does not necessarily result in higher extraction. Ore 1 had the lowest nickel grade but achieved the highest extraction of Ni (97.25%) and Co (98.49%) under experimental conditions using an acid-to-ore (A/O) ratio of 0.40. This significant Ni extraction is attributed to nickel's structural substitution in goethite, an iron oxide mineral that dissolves readily under the HPAL process. Ore 2 also contains goethite as the dominant phase and achieved similarly high recoveries of Ni (97%) and Co (98%), however, Co recovery decreased slightly under higher acid conditions due to co-precipitation with hematite. Ore 3 had the highest nickel grade but the lowest leaching efficiency (<90% Ni). The generally low recoveries may be attributed to nickel being hosted in both goethite (a leachable phase) and lizardite (a less leachable phase). The silicate matrix of lizardite and its elevated magnesium content restricted the effective acid range and thus diminished nickel selectivity during the HPAL leaching process.

The results highlight that the mineralogical occurrence state of nickel is more important than nickel grade in determining leaching performance. Therefore, low-grade limonite ores with favorable mineralogy can serve as potential feed sources for environmentally friendly sustainable nickel hydrometallurgical extraction.

Keywords: *Lateritic nickel ore; Leaching behavior; Recovery efficiency; Limonite; Saprolite*

1. Introduction

Nickel is an essential metal extensively utilized in industries such as stainless steel manufacturing, battery production, and the high-performance alloys due to its excellent corrosion resistance and ability to withstand high temperatures [1, 2, 3]. The surge in nickel demand, driven by the expansion of electric vehicle markets and renewable energy technologies, with projected to rise from around 7% in 2021 to 40% by 2040, has significantly intensified the need for efficient extraction methods from nickel ores [4, 5].

Historically, nickel extraction has primarily focused on sulfide ores which are found in countries such as Canada, the USA, and Australia [6]. However, the depletion of high-grade sulfide deposits over the past two decades has shifted attention toward laterite ore, which account for more than 70% of the world nickel reserves [7, 8]. Nickel laterite ores are formed through the extensive weathering of ultramafic rocks and are primarly concentrated in tropical and subtropical regions, generally situated within 22 degrees of latitude both north and south of the equator [9]. Generally, laterite is categorized into two main types based on mineralogical composition and chemical properties: Saprolite, rich in magnesium silicates and Limonite, dominated by iron oxides and hydroxides [10].

The existing literature has thoroughly established the broad mineralogical and metallurgical differences between saprolite and limonite. Saprolite ores contain higher nickel concentrations, ranging from 1.5% to 3% and are associated with magnesium silicate minerals such as lizardite and garnierite [11]. These ores are primarily processed through energy-intensive pyrometallurgical methods to produce valuable nickel products such as ferronickel, nickel matte and nickel pig iron [12, 13]. In contrast, limonite ores, which have moderate nickel grades ranging from 0.6% to 1.5%, are rich in iron oxides and hydroxides and serve as a

Corresponding author: aliefrasyidibaking@gmail.com

https://doi.org/10.2298/JMMB250308028B

key raw material for electric vehicle battery cathodes [14, 15]. Hydrometallurgical plants typically utilize limonite with a nickel content above 1%, leaving ultra-low-grade limonite (<1% Ni) largely [16].

The exclusion of ultra-low limonite from industrial processing presents several disadvantages. First, it results in suboptimal utilization of mineral resources, as potentially nickel that is found in goethite [17]. Second, neglecting this ore contributes to greater environmental degradation by increasing waste accumulation and land disturbance [18]. Third, it minimizes the economic value of mining operations, particularly in rich resources regions where local beneficiation of all ore grades could support regional development [19]. Finally, failure to utilize ultra-low limonite ores increases dependence on the higher grade deposits, which may lead to their rapid depletion and pose challenges for ensuring a stable nickel supply over time.

Although numerous studies such us Stankovic et al. (2020) and Deniyatno et al. (2022) have widely investigated the leaching mechanisms of lateritic nickel ore through high-pressure acid leaching and atmospheric [20, 21], few have directly compared how nickel grade and nickel occurrence state respectively influence leaching behavior under identical processing. The comparison result is crucial to explain whether the nickel dissolution is primary governed by nickel amount, or by nickel mineralogical bound. Some study explain that goethite rich nickel ore is more reactive, and others highlight that nickel silicate lattice requires higher acid dose and longer time. However, the conclusions drawn are often based on ore samples with differing origins and experimental conditions, thereby limiting their comparability.

This study aims to fill that critical gap by systematically evaluating the influence of both nickel grade and occurrence state on the HPAL leaching performance of three distinct lateritic ores that are ultra- low limonite, limonite, and saprolite**.** Through comprehensive mineralogical characterization (XRD, SEM-EDS, EPMA) and controlled leaching experiments at 250 °C, this allows direct comparison of Ni extraction efficiency as a function of grade and host phase. This work is the first to decouple these two critical variables under unified experimental control, providing insight into process optimization and supporting the sustainable utilization of underused ultra-low limonite resources.

2. Materials and methods

2.1. Materials

In this investigation, three distinct types of lateritic nickel ores were employed: ultra-low limonite (ore 1), limonite (ore 2), and saprolite (ore 3). The strategic selection of these specific ore types was intended to examine how variations in nickel content and inherent mineralogical characteristics influence leaching mechanisms. The ore 1, 2, and 3 were procured from PT. Almharig, Kabaena Island, Indonesia. The chemical compositions of these ores were analyzed using Inductive couple plasma – optical emission spectrometry (ICP-OES) and illustrated in Table 1. Before the leaching experiments, samples of the three nickel ores were prepared by drying them at 105°C for 24 hours to remove all moisture. The dried ores were sequentially crushed using a jaw crusher, a drum mill for uniform particle size, and a pulverizer mill for finer particles. Finally, the ground ore was sifted through a 100-mesh sieve to ensure consistency in particle size for the leaching tests. The leaching agent used in this study was industrial-grade sulfuric acid, sourced from QMB Indonesia and produced by Merdeka Tsingshan Indonesia (MTI). Sulfuric acid plays a crucial role in leaching by effectively dissolving the nickel from the lateritic ores and facilitating its extraction [22].

2.2. Leaching experiment

A mixture of 300 g nickel ore and 700 mL distilled water was prepared in a 2 L beaker and stirred for 20 minutes to form a slurry. Sulfuric acid was added during the final 10 minutes to achieve acid-to-slurry ratios of 0.25:1, 0.30:1, 0.35:1, and 0.40:1, resulting in a total slurry volume of approximately 1.0–1.1 L, which is fully compatible with the 2 L beaker. The initial solids content was about 30 wt.%, and this percentage decreased slightly after acid addition due to dilution. The slurry was then transferred to a 2 L autoclave and subjected to leaching at 250 °C for 60 minutes. After the leaching process, the liquid and

Table 1. *Mineral composition of the ore samples*

Ore	Content (wt.%)						
	Ni	**Co**	**Mn**	**Fe**	**Al**	**Mg**	**SiO_2**
1	0.733	0.066	0.432	37.09	4.56	0.405	18.71
2	1.34	0.073	0.616	41.64	3.01	1.26	12.96
3	2	0.082	0.568	17.42	3.2	5.17	34.39

solid phases were separated by vacuum filtration, and the solid residue was washed three times with distilled water to remove impurities before being dried at 105 °C for 12 hours for subsequent analysis.

2.3. Analytical methods

The concentration of solutions and solid samples were analysed using Inductive couple plasma – optical emission spectrometry (Spectro Arcos). Solid samples from ore and leaching residue were characterized using X-ray diffraction (Rigaku), mineral liberation analysis (Thermo Scientific) and electron probe microanalyzer (8050G Shimadzu).

3. Results and discussion

3.1. Characterization of the ore

3.1.1. Mineralogical analyses of the ore 1

Ore 1 was comprehensively characterized using ICP, XRD, SEM, and EPMA analyses to evaluate its chemical composition and mineralogical features in detail. The ICP results (Table 1) indicate that iron (37.09%) is the dominant constituent of the ore, accompanied by substantial amounts of silica (18.71%), aluminum (4.56%), and magnesium (0.405%), which together suggest a mixed iron oxide–silicate matrix typical of weathered lateritic profiles. Nickel (0.733%) and cobalt (0.066%) occur at low levels, consistent with the characteristic geochemical signature of limonitic laterites where these metals are usually dispersed within iron oxyhydroxides or adsorbed onto secondary mineral surfaces.

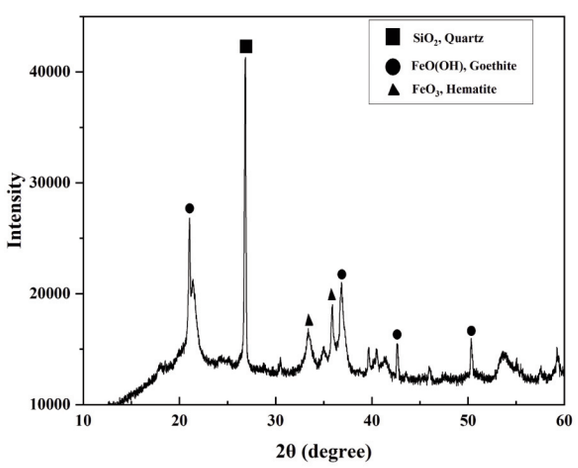

Figure 1. *XRD analysis of ore 1*

The XRD analyses of ore 1 in Figure 1 shows that the ore is dominated by goethite (FeOOH), and quartz, with a minor of hematite. A clear peak of goethite represents the excessive amount of iron also the intense peaks for quartz reflect significant crystalline silica content. The minor presence of hematite further confirms the extensive degree of weathering experienced by the ore, indicating highly oxidizing and intensely leached conditions typical of limonitic profiles [24, 25]. The following Figure 2 presents SEM-BSE micrographs of the ore, revealing the spatial distribution and morphology of its principal mineral phases, including hematite, goethite, olivine, kaolinite, and quartz. As show in figure 2-A, pixel-brightness contrast delineates two distinct zones, the brighter zone corresponding to Fe-rich phases (hematite and goethite) and darker zone representing to silicate minerals (olivine, kaolinite, and quartz). Figure 2-B further confirms that nickel is concentrated within the bright Fe- rich domain, indicating its preferential incorporation into iron oxides. This association is consistent with the close ionic radii of Fe^{3+} and Ni^{2+}, which facilitate isomorphous substitution of Ni into the goethite lattice [26].

The figure 3, EPMA analysis of Ore 1 reveals that iron (Fe), at a concentration of 9.7%, is the dominant element, confirming goethite (FeOOH) as the primary mineral phase. Nickel (3.8%) is closely associated with iron, as demonstrated by their co-localization in the marked regions, indicating that nickel is either structurally incorporated into the goethite lattice or adsorbed onto its surface. This close association makes nickel more accessible during leaching processes that target goethite dissolution [27]. Silicon (3.7%) and aluminum (2.7%) are distributed uniformly across the sample, suggesting the presence of quartz and aluminosilicate phases, respectively. In contrast, magnesium (1.2%) and calcium (3.5%) appear in localized regions, likely originating from minor silicate. These findings underscore the role of goethite as the primary host for nickel in this ore and highlight the importance of optimizing leaching parameters to maximize nickel extraction while effectively managing refractory phases such as quartz.

3.1.2. Mineralogical analyses of the ore 2

Ore 2, classified as iron-rich limonite, exhibits a high iron content of 41.64% based on ICP analysis, in Table 1 with a moderate nickel concentration of 1.34% and trace levels of cobalt (0.073%) and manganese (0.616%), suggesting potential metallurgical value. The silica content of 12.96% indicates quartz impurities, while aluminum (3.01%) and magnesium (1.26%) suggest contributions from serpentine minerals, reflecting the complex mineralogy of the deposit.

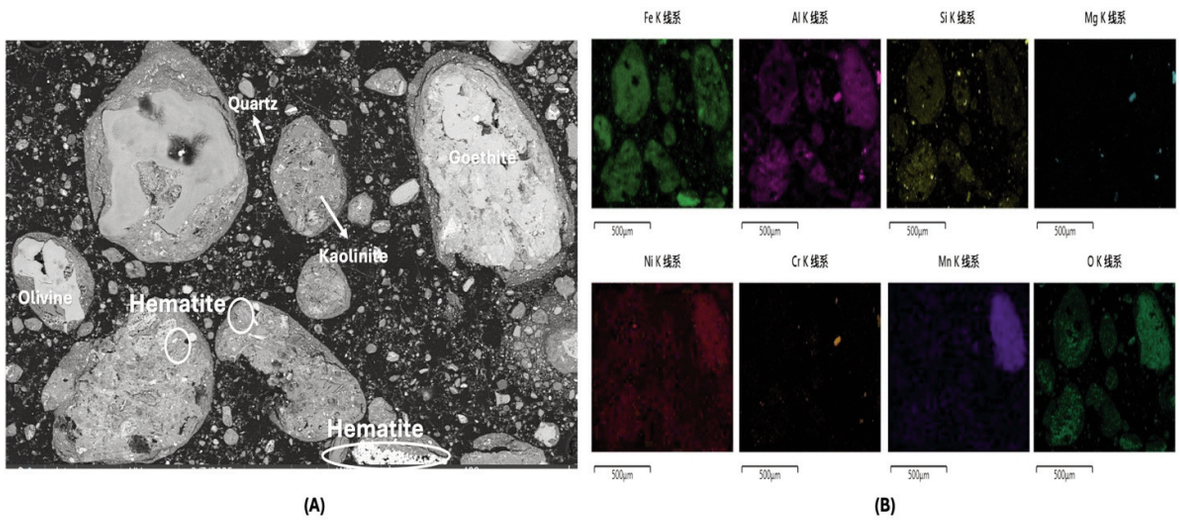

Figure 2. *The ore 1 of (A) BSE analysis (B) elemental mapping*

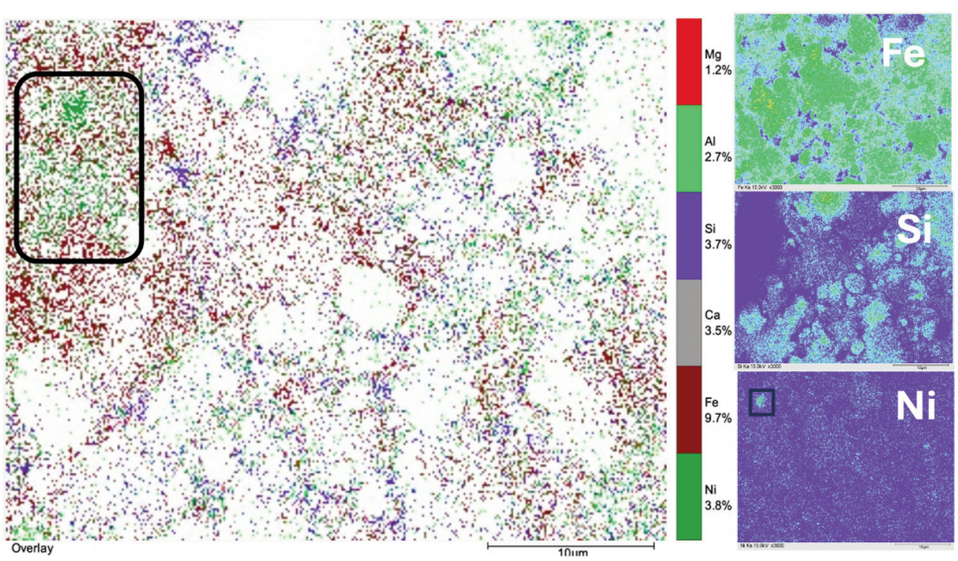

Figure 3. *EPMA analysis of ore 1*

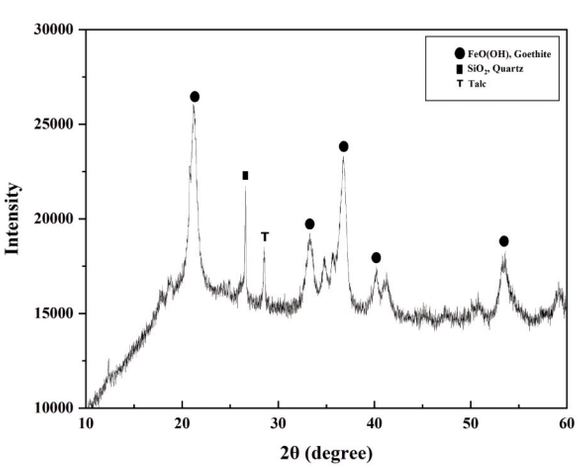

Figure 4. *XRD analysis of ore 2*

XRD analysis in figure 4 confirms goethite as the dominant iron-bearing phase, typical of limonite ores, with quartz as a major impurity. Unlike Ore 1, which contains hematite due to surface-level dry oxidation, Ore 2 lacks hematite, indicative of its formation under hydrated and leaching-dominant conditions. The minor presence of talc suggests secondary weathering processes or localized enrichment of silicate minerals. Figure 5 shows that the central large grain is primarily composed of talc, identified by its darker shade in the BSE image (figure 5-A) and supported by significant Mg and Si concentrations (figure 5-B). Surrounding this grain, goethite is observed as brighter phases due to its higher iron content, confirmed by intense Fe and O signals. Elemental mapping clearly differentiates the silicate-rich talc from iron-rich goethite by their

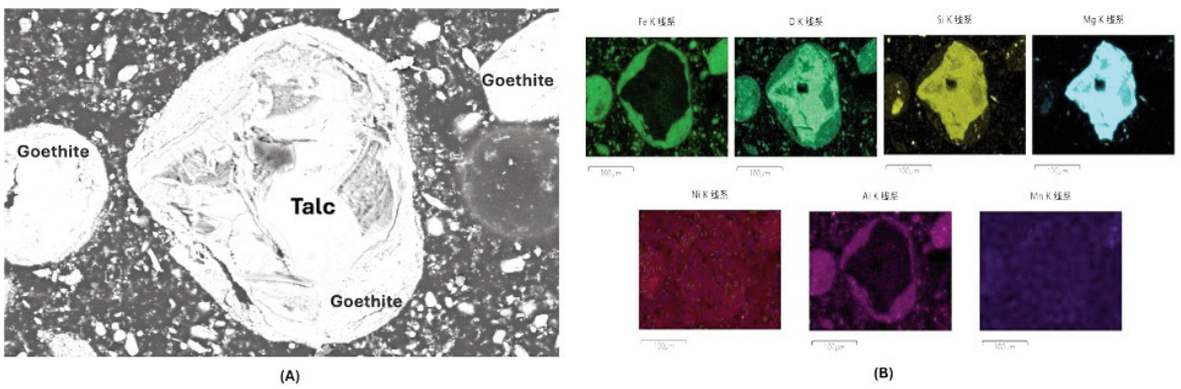

Figure 5. *The ore 2 of (A) BSE analysis (B) elemental mapping*

unique elemental signatures, with Mg and Si strongly concentrated within the talc, while Fe is predominantly confined to goethite regions. The Ni elemental map indicates a subtle, yet consistent presence of nickel primarily associated with the Fe-rich goethite areas, suggesting substitution of Ni into the goethite lattice or adsorption onto its surface. Nickel signals are weak to absent in the talc grain, emphasizing limited substitution or absence of Ni within magnesium-silicate structures in this ore.

In Figure 6 the sample was observed by EPMA, the distribution of nickel spreads across the ore surface, closely following the dispersion of iron. This is further highlighted in the circled area, where the overlay shows nickel represented in a specific color overlapping with the gray region that denotes iron, indicating their association. Overlay mapping indicates nickel's structural incorporation within goethite due to the similarity in ionic radii (Ni^{2+} ~0.69 Å, Fe^{3+} ~0.64 Å), despite their different valences [28, 29].

3.1.3. Mineralogical analyses of the ore 3

Ore 3 exhibits a distinct composition and mineralogical structure, as determined through ICP, EDX, XRD, and EPMA analyses. ICP results in table 1 reveal a high nickel content (2.00%) alongside moderate cobalt (0.082%) and manganese (0.568%) concentrations, with a relatively low iron content (17.42%), diverging from the composition of typical lateritic ores. The high silicon dioxide (34.39%) and magnesium (5.17%) concentrations suggest the dominance of silicate minerals, particularly hydrous silicates such as lizardite, a key component of serpentinized ultramafic rocks. Aluminum (3.20%) further indicates the presence of aluminosilicate phases.

XRD results (Figure 7) indicate that lizardite, $Mg_3(Si_2O_5)(OH)_4$, was the most abundant phase identified, with significant quartz reflections and moderate goethite peaks. The abundance of lizardite confirmed the high Mg and Si contents obtained by ICP for the saprolitic ore, while the lower concentrations of

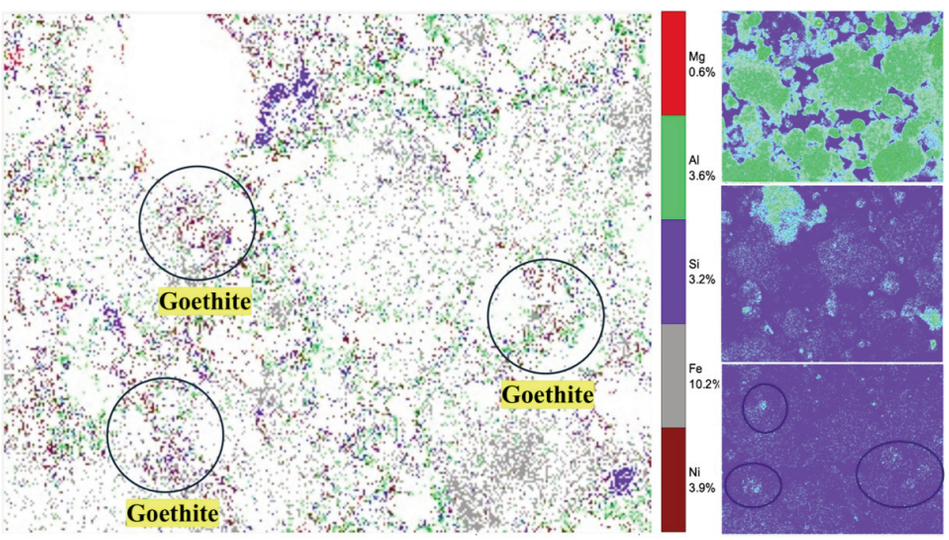

Figure 6. *EPMA analysis of ore 2*

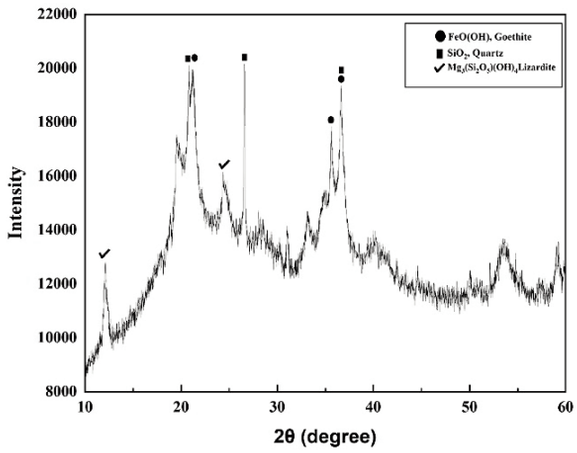

Figure 7. *XRD analysis of ore 3*

Fe confirmed the smaller goethite signal relative to the previous two ores. The SEM-BSE micrograph of Ore 3 results in Figure 8 indicated a predominance of dark areas indicating silicate minerals (lizardite, talc and quartz), with only limited examples of bright, Fe-rich areas indicating only limited examples of goethite. Further, the elemental mapping shown in Figure 8-B indicated that nickel was enriched in both bright and dark areas, indicating that Ni was partitioned not only into the goethite but also into the lizardite matrix. This dual host-phase affinity coupled with its higher Overall content explains the higher overall nickel content of Ore 3 in comparison to the first two ores and supports the mineralogical interpretations from bulk chemical and XRD data.

EPMA analysis (Figure 9) provides a detailed understanding of nickel distribution in Ore 3, revealing its complex association with both silicate and iron oxide phases. Iron (Fe) displays a uniform distribution across the image, while magnesium (Mg) is concentrated primarily in the top-left corner and partially in the center. Nickel (Ni) mirrors these patterns, appearing in regions enriched with either iron or magnesium, indicating a dual association with goethite and lizardite. Ore 3 shows a stronger linkage to silicate phases—particularly lizardite. This is attributed to the similar ionic radii of Ni^{2+} and Mg^{2+}, which enables isomorphic substitution and facilitates nickel incorporation into the silicate structure [30]. Consequently, Ore 3 is characterized as saprolitic due to its high silica content, low iron levels, and unique mineralogical composition, all of which significantly influence its leaching behavior.

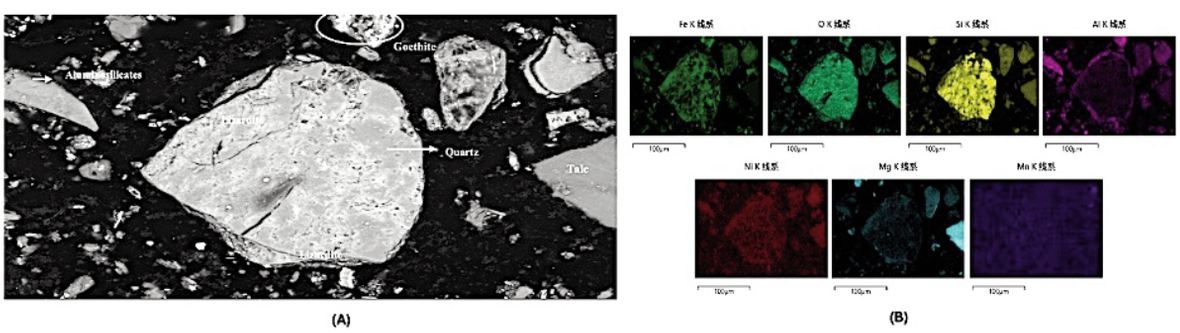

Figure 8. *The ore 3 of (A) BSE analysis (B) elemental mapping*

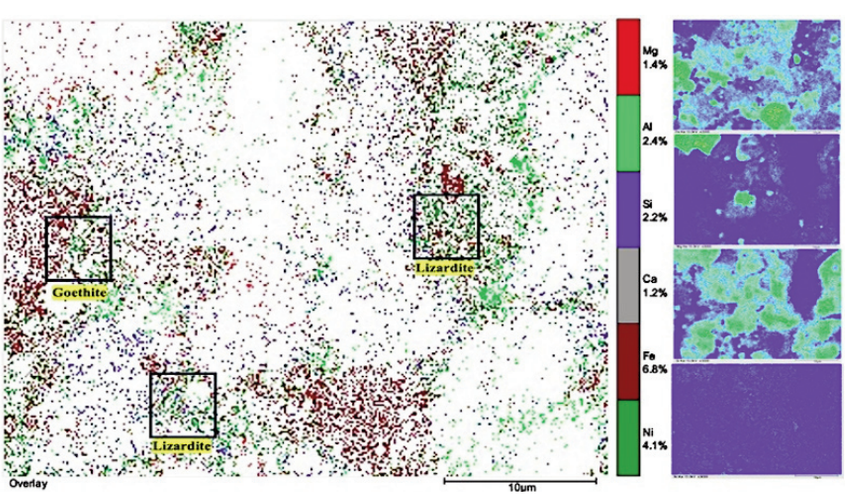

Figure 9. *EPMA analysis of ore 3*

3.1.4. Leaching Performance

High-pressure acid leaching (HPAL) of Ore 1 at 250 °C in Figure 10-A demonstrates a marked increase in nickel and cobalt extraction efficiency with increasing acid-to-ore (A/O ratio). Maximum nickel (97.25%) and cobalt (98.49%) recoveries are achieved at an A/O ratio of 0.40. For comparison, iron dissolution is greatly suppressed, stabilizing at approximately 10%, which is beneficial for purification downstream. In terms of aluminum and magnesium, due to the more stable aluminosilicate and silicate phases, both metals show slower leaching kinetics with respective recoveries of 45.43% and 75.85% The XRD patterns in Figure 10-B further support these observations, where the goethite peaks corresponding to the same characteristic reflections previously identified in Figure 2 progressively decrease in intensity as the leaching temperature increases. This systematic reduction in peak intensity clearly reflects the gradual dissolution of the iron bearing goethite phase, which is known to act as a major host for nickel and cobalt in limonitic laterites. As the goethite structure breaks down, the lattice bound nickel and cobalt incorporated within its crystal framework are liberated into the leach solution, thereby contributing to the increased extraction efficiencies. The disappearance of the goethite peaks and the appearance and increasing intensity of new hematite peaks demonstrate that dissolved iron ions are re-precipitating as hematite. The quartz peaks remain throughout treatment time suggesting it was chemically inert in these conditions. The appearance of alunite in association with higher A/O ratio also indicates secondary precipitation as dissolved aluminum and sulfate are involved. All this observation shows that successful leaching of Ni and Co from Ore 1 is a process that relates to the breakdown of goethite but with iron re-precipitation occurring as hematite to help limit the Fe contamination of the leachate.

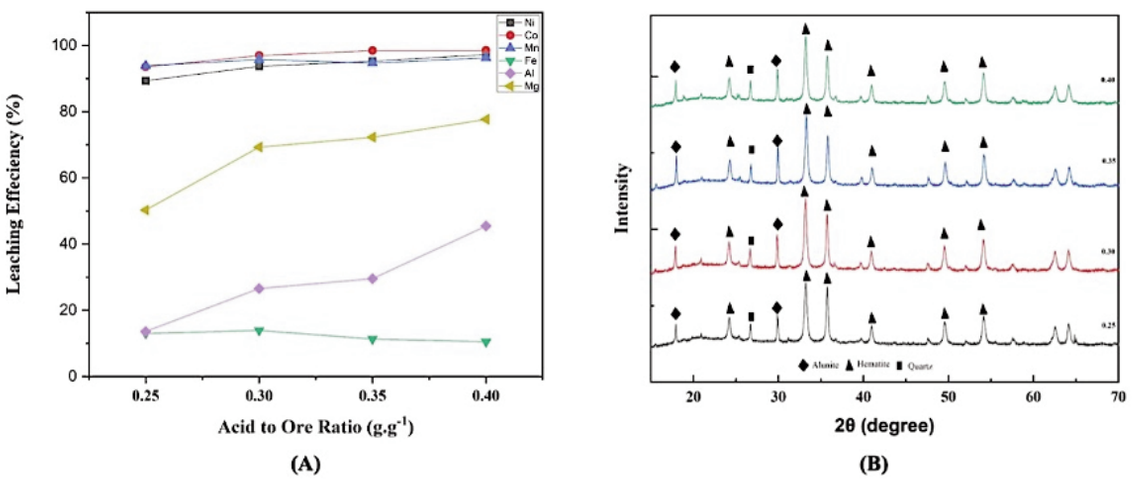

Figure 10. *(A) HPAL efficiency of ore 1; (B) XRD analysis of ore 1 after HPAL*

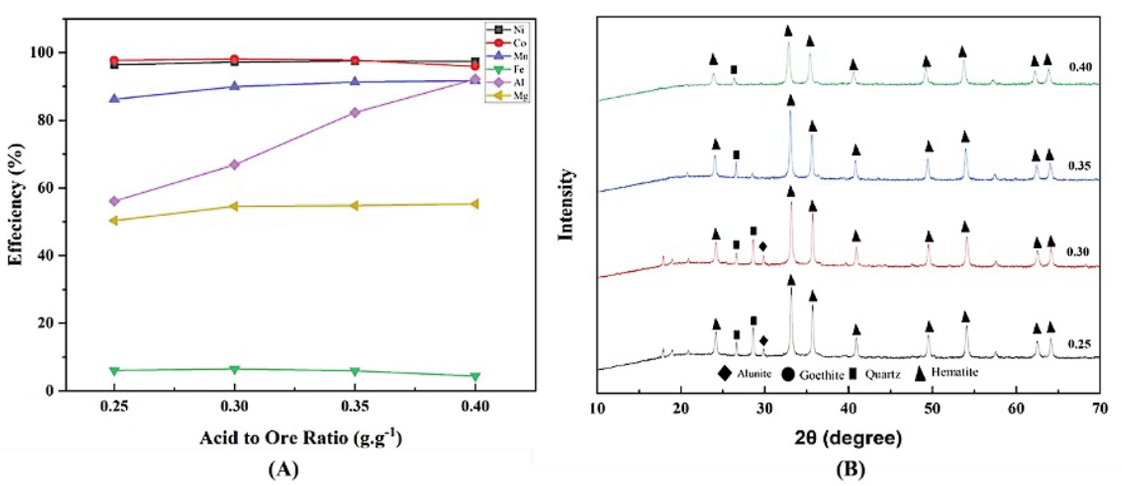

Figure 11. *(A) HPAL efficiency of ore 2 (B) XRD analysis of ore 2 after HPAL*

Ore 2 demonstrates excellent leaching performance for nickel HPAL conditions (Figure 11-A), with recovery of 97.00% nickel at an A/O of 0.30 and supported further acid additions without loss of stability. Mn, Al and Mg also show increased recoveries as acid increases, consistent with their acid-soluble disposition. Dissolution of iron remained low (<10%) indicating good selectivity, but cobalt recovery dropped slightly from 98.00% to 95.92% as A/O increased. This is likely due to co-precipitation with hematite; during hydrolysis of Fe^{3+}, solid hematite can form which might trap Co and reduce availability for extraction [31]. The HPAL residue was analyzed with XRD (Figure 11-B) to confirm goethite had been dissolved (the goethite peaks disappeared, and hematite peaks dominated) and Quartz is unchanged. The conversion of goethite promotes the effective extraction of Ni, but the primary product is the formation of hematite which could entrap Co and other trace metals.

As shown in Figure 12-A, Ore 3 shows significantly poorer leaching performance compared with Ores 1 and 2. The nickel recovery is less than 90% at an A/O ratio of 0.40, and the recoveries of cobalt and manganese also decrease to below 95% and 90%, respectively. The recovery of aluminum remains low, indicating its tendency to precipitate, whereas magnesium dissolution follows a trend similar to nickel. This behavior can be attributed to the co-occurrence of nickel and magnesium within similar silicate mineral families, dominated by lizardite-type phases. However, the higher magnesium content in the pregnant leach solution reduces nickel selectivity in downstream separation processes and necessitates additional impurity removal steps. There is limited iron extraction for lower acid ratios (0.25-0.30), around 2% total iron extraction. However, eventually the total iron extraction slowly rose to 4.17% and then finally 6.71% total iron extraction at A/O of 0.35 and 0.40 ratios respectively. This gradual increase suggests that goethite dissolution is ongoing and incomplete at these conditions, consistent with partial dissolution rather than immediate precipitation. The corresponding XRD image in Figure 12-B illustrates these leaching observations. The transformation of lizardite is total, though the ongoing presence of crystalline peaks from goethite at A/O 0.25 indicates that the saprolitic ore matrix has yet to be destroyed. This incomplete destruction means nickel is not liberated adequately that is a possible explanation for the lower leaching efficiency. As goethite dissolves, hematite begins to form due to hydrolysis and re-precipitation of the Fe^{3+} ions. As this occurs, magnesium is leached from lizardite, while unreactive silica forms in the solid state residue, because of lizardite breakdown. At A/O 0.35 alunite was formed in dissolution, as the pH and the concentrations of Al^{3+}, Fe^{3+}, and SO_4^{2-} ions in solution increased. This supports the reduction in aluminum recovery gradient, further suggesting that aluminum must have been immobilized into stable secondary phases. Ultimately, the mineralogical complexity of Ore 3 and any impurity load in the leachate demonstrates a further need for increased process control and selective removal of impurities as to maximize the possible recovery of Ni.

4. Discussion

4.1. Influence of nickel grade on leaching

To evaluate the effect of nickel grade on leaching performance, three lateritic nickel ores that differ in Ni grades were tested using high-pressure acid leaching (HPAL): Ore 1 (ultra-low limonite, 0.73 wt.% Ni), Ore 2 (limonite, 1.34 wt.% Ni) and Ore 3 (saprolite, 2.00 wt.% Ni). They were tested using increasing acid-to-ore (A/O) ratios. The results show that higher nickel grade does not equate to better leaching performance.

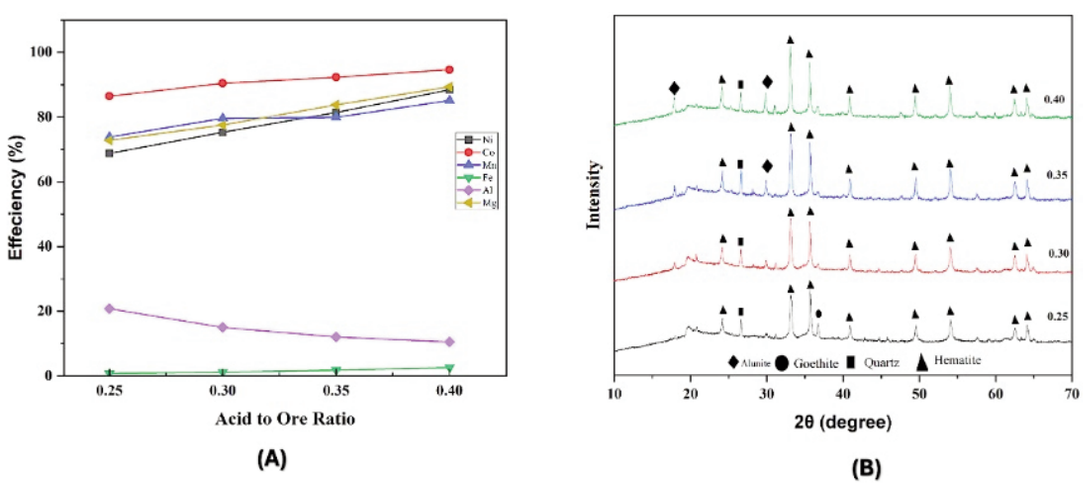

Figure 12. *(A) HPAL efficiency of ore 3 (B) XRD analysis of ore 3 after HPAL*

Despite the appreciable lower nickel content, Ore 1 achieved the great nickel recovery (97.25%) and cobalt recovery (98.49%) at an A/O ratio of 0.40. Ore 2, having a moderately higher nickel grade, provided excellent recoveries, 97% Ni and 98% Co at a lower A/O of 0.30, although it did experience a reduction in Co recovery at higher acid addition due to the influence of secondary precipitation processes.

In contrast, despite possessing the highest nickel content (2.00 wt.%), Ore 3 demonstrated the lowest extraction efficiency, with nickel recovery not exceeding 90% and cobalt less than 95% at the highest acid dosage. This inefficiency is likely related to the complexity the saprolite mineralogy, with the presence of magnesium silicate minerals, such as lizardite, being more resistant to acid attack and consuming longer reaction times or higher leaching conditions. Furthermore, the presence of significant dissolved magnesium in the pregnant leach solution limits nickel selectivity and increases purification burden downstream. From this data, it also suggests that leaching efficiency under HPAL does not directly correlate with nickel grade. While Ni concentration is an important resource evaluation, leaching efficiency appears to be directly influenced by additional variables, such as mineralogical classification, mineral phase reactivity, and impurity dissolution. While these results are preliminary, they demonstrate that nickel grade does not allow for fair prediction of leaching, and ultimately highlight the need to characterize how nickel is hosted by the ore matrix, which is addressed in the following discussion regarding the state of nickel occurrence.

4.2. Influence of nickel occurrence on leaching behaviour

The leaching behavior of nickel in lateritic ores is governed not only by its total concentration but critically by the mineral phases in which it resides. Ore 1 (ultra-low limonite) and Ore 2 (limonite) generally hosts nickel as goethite with Ni^{2+} ions substituting for Fe^{3+} in the goethite lattice because ionic radii for both ions are similar. Dissolution in HPAL conditions show in Figure 13-A, protons (H^+) from sulfuric acid deconstruct the goethite lattice and dissolve the mineral (reaction 1), releasing Fe^{3+}, Ni^{2+}, and Co^{2+} to the leachate (reaction 2-4). As temperature in the HPAL process increases above 130 °C, the Fe^{3+} precipitates as hematite (reaction 5), minimizing Fe contamination of the pregnant leach solution (PLS). This sequential mechanism, in which goethite dissolves first and hematite subsequently precipitates, effectively suppresses iron contamination and enhances nickel selectivity. The low iron extraction (<10%) and high nickel recovery (>97%) observed in the experiments are fully consistent with this behavior. Collectively, these results clearly demonstrate that nickel hosted in goethite is highly reactive and exhibits fast leaching kinetics under HPAL conditions.

$$H_2SO_4 \rightarrow 2H^+ + SO_4^{2-} \quad (1)$$

$$FeOOH + 3H^+ \rightarrow Fe^{3+} + 2H_2O \quad (2)$$

$$NiO + 2H^+ \rightarrow Ni^{2+} + H_2O \quad (3)$$

$$CoO + 2H^+ \rightarrow Co^{2+} + H_2O \quad (4)$$

$$2Fe^{3+} + 3H_2O \rightarrow 3Fe_2O_3 + 6H^+ \quad (5)$$

$$Mg_3Si_2O_5(OH)_4 + 6H^+ \rightarrow 3Mg^{2+} + 2SiO_2 + 5H_2O \quad (6)$$

In contrast, Ore 3 is a saprolitic ore with a higher nickel grade, where nickel is predominantly hosted within magnesium-silicate minerals, primarily lizardite, with only minor contributions from residual goethite. XRD patterns and SEM–EDS mapping confirms a dual mode of nickel association, as Ni

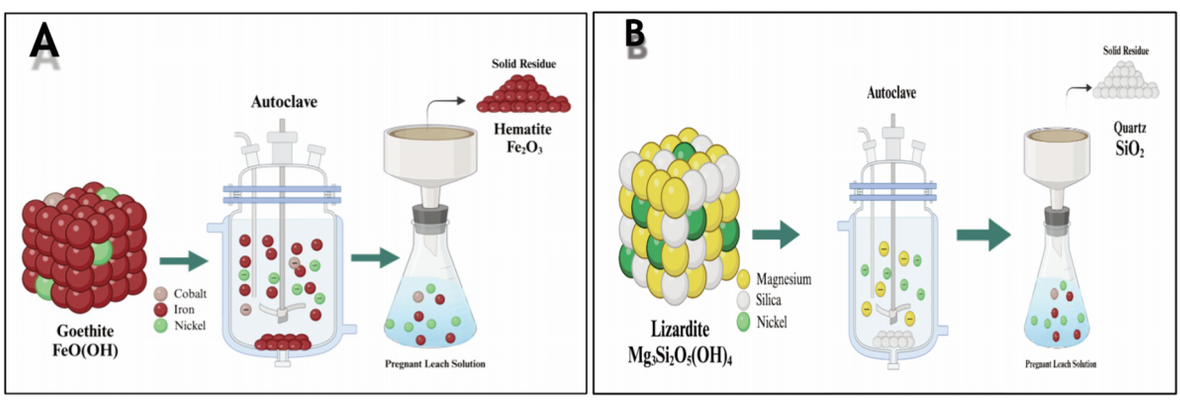

Figure 13. *Dissolution behavior of laterite by the approach of (A) goethite (B) lizardite*

appears in both silicate-rich (dark) and iron-rich (bright) regions. Nickel release from lizardite, as shown in Figure 13-B, occurs through a proton-exchange dissolution mechanism in which H^+ ions attack the Mg–O and Ni–O bonds in the phyllosilicate structure (Reaction 6). This process liberates Mg^{2+} and Ni^{2+} into solution while leaving the SiO_2 framework largely intact. Despite this mechanism, the overall leaching efficiency remains limited due to two primary constraints. The first is the structural stability and inherently low reactivity of silicate phases such as lizardite, which substantially slows the dissolution rate. The second is the high magnesium content of the ore, which competes strongly with nickel for the available acid, consuming large quantities of H^+ and reducing the acid available to dissolve nickel. This competition significantly increases total acid demand and ultimately diminishes nickel selectivity during the leaching process.

These findings show that the mineralogical mode of nickel occurrence, rather than its grade, is the primary factor governing HPAL leachability. Nickel hosted in iron-oxyhydroxides such as goethite is readily liberated as the Fe structure hydrolyzes, enabling high extraction and cleaner impurity separation. By contrast, nickel bound within silicate phases like lizardite is far less reactive, requiring harsher conditions and leading to substantial co-dissolution of Mg, Si, and Al, which increases acid demand and reduces process selectivity. Therefore, effective HPAL process design must be guided by detailed mineralogical characterization to identify the dominant nickel-bearing phases and anticipate their dissolution behavior.

5. Conclusion

The comparative assessment of the three lateritic nickel ores demonstrates that HPAL leaching performance is governed primarily by the mineralogical mode of nickel occurrence rather than nickel grade itself. Ore 1, although containing a low nickel grade (0.73 wt%), achieved the high extraction efficiency and strong selectivity because its nickel is predominantly hosted in goethite, a phase that dissolves readily under HPAL conditions while suppressing iron co-dissolution, and this favorable mineralogy indicates that such low-grade limonitic ores can still serve as viable and sustainable HPAL feedstocks when selectivity and impurity control are prioritized. Ore 2, with a moderate nickel grade (1.34 wt%), also performed well, maintaining good recovery and selectivity across increasing acid additions due to its mixed but still largely acid-soluble mineral assemblage. Ore 3 contained the highest nickel grade (2.00 wt%) but exhibited the poorest extraction behavior because most of its nickel is structurally bound within magnesium-silicate minerals such as lizardite, which dissolve slowly and consume large amounts of acid due to their high magnesium content.

These results clearly show that higher nickel grade does not necessarily translate to better leaching performance. Instead, the mineralogical form in which nickel is hosted, whether within iron oxyhydroxides or within silicate frameworks, determines dissolution kinetics, acid demand, impurity co-dissolution, and overall process efficiency. Therefore, detailed mineralogical characterization is essential for evaluating ore suitability and designing effective HPAL operating strategies for lateritic nickel resources.

Acknowledgements

Aad Alief Rasyidi Baking conducted the experiments, performed data analysis, and prepared the original draft of the manuscript. Zhou Lejun provided overall supervision and critically reviewed the manuscript. Liu Wei contributed to the review of the experimental design and provided scientific supervision throughout the study. All authors have read and approved the final manuscript.

Author's contributions

Aad Alief Rasyidi Baking conducted the experiments, performed data analysis, and prepared the original draft of the manuscript. Zhou Lejun provided overall supervision and critically reviewed the manuscript. Liu Wei contributed to the review of the experimental design and provided scientific supervision throughout the study. All authors have read and approved the final manuscript.

Data availability

The data supporting the findings of this study are openly available and can be accessed upon reasonable request.

Conflict of interest

The authors declare that this study was supported by joint funding under the Indonesia–China Metallurgy Scholarship Cooperation Program involving the Indonesia Endowment Fund for Education (LPDP), GEM Co., Ltd., and Central South University. The funding organizations had no involvement in the study design, data collection, data

analysis, interpretation of results, or the decision to publish the manuscript.

References

[1] G. Mudd, S. Jowitt, A detailed assessment of global nickel resource trends and endowments, Economic Geology, 109 (7) (2014) 1813–1841. https://doi.org/10.2113/econgeo.109.7.1813

[2] S. A. Farooq, A. Raina, M. I. Ul Haq, A. Anand, Corrosion behaviour of engineering materials: A review of mitigation methodologies for different environments, Journal of The Institution of Engineers (India): Series D, 103 (2) (2022) 639–661. https://doi.org/10.1007/s40033-022-00367-5

[3] E. Cattaneo, B. Riegel, Chemistry and electrochemistry | nickel, in Encyclopedia of Electrochemical Power Sources, J. Garche (Ed.), Elsevier, Oxford, 2025, p. 740–761.

[4] F. Maisel, C. Neef, F. Marscheider-Weidemann, N. F. Nissen, A forecast on future raw material demand and recycling potential of lithium-ion batteries in electric vehicles, Resources, Conservation and Recycling, 192 (2023) 106920. https://doi.org/10.1016/j.resconrec.2023.106920

[5] A. I. Volkov, D. V. Zhuzhel'skii, E. G. Tolstopyatova, V. V. Kondratiev, Synthesis and electrochemical research of the properties of mixed nickel-cobalt oxides as materials for energy storage devices, Russian Journal of Applied Chemistry, 93 (12) (2020) 1837–1844. https://doi.org/10.1134/S1070427220120058

[6] F. Wang, F. Liu, R. Elliott, S. Rezaei, L. T. Khajavi, M. Barati, Solid state extraction of nickel from nickel sulfide concentrates, Journal of Alloys and Compounds, 822 (2020) 153582. https://doi.org/10.1016/j.jallcom.2019.153582

[7] A. Vahed, P. Mackey, A. Warner, Around the nickel world in eighty days: A virtual tour of world nickel sulphide and laterite operations and technologies, in Handbook of Extractive Metallurgy, Springer, Berlin, 2021, p. 3–39. https://doi.org/10.1007/978-3-030-65647-8_1

[8] Z. Zhang, W. Zhang, Z. Zhang, X. Chen, Nickel extraction from nickel laterites: Processes, resources, environment and cost, China Geology, 8 (1) (2025) 187–213. https://doi.org/10.31035/cg2024124

[9] Y. Zhang, J. Qie, X.F. Wang, K. Cui, T. Fu, J. Wang, Y. Qi, Mineralogical characteristics of the nickel laterite, Southeast Ophiolite Belt, Sulawesi Island, Indonesia, Mining, Metallurgy & Exploration, 37 (1) (2020) 79–91. https://doi.org/10.1007/s42461-019-00147-y

[10] K. Aquino, C. Arcilla, C. Tupaz, C. Schardt, Mineralogical and geochemical characterization of the Sta. Cruz nickel laterite deposit, Zambales, Philippines, Minerals, 12 (3) (2022) 305. https://doi.org/10.3390/min12030305

[11] S. Sufriadin, A. Idrus, S. Pramumijoyo, I. Warmada, A. Imai, Study on mineralogy and chemistry of the saprolitic nickel ores from Soroako, Sulawesi, Indonesia: Implication for the lateritic ore processing, Journal of Applied Geology, 3 (2011) 23–33. https://doi.org/10.22146/jag.7178

[12] J. Xiao, W. Xiong, K. Zou, T. Chen, H. Li, Z. Wang, Extraction of nickel from magnesia–nickel silicate ore, Journal of Sustainable Metallurgy, 7 (2) (2021) 642–652. https://doi.org/10.1007/s40831-021-00364-0

[13] E. Urtnasan, S.-B. Heo, J.-W. Yu, C.-H. Jung, J.-P. Wang, Relationship between thermodynamic modeling and experimental process for optimization ferro-nickel smelting, Minerals, 15 (2) (2025) 101. https://doi.org/10.3390/min15020101

[14] M. Rao, J. Chen, T. Zhang, M. Hu, J. You, J. Luo, Atmospheric acid leaching of powdery Ni–Co–Fe alloy derived from reductive roasting of limonitic laterite ore and recovery of battery grade iron phosphate, Hydrometallurgy, 218 (2023) 106058. https://doi.org/10.1016/j.hydromet.2023.106058

[15] F. Wang, D. Dreisinger, An integrated process of CO_2 mineralization and selective nickel and cobalt recovery from olivine and laterites, Chemical Engineering Journal, 451 (2023) 139002. https://doi.org/10.1016/j.cej.2022.139002

[16] M. Fatahi, N. Mohammad, S. Ziaeddin, Nickel extraction from low grade laterite by agitation leaching at atmospheric pressure, International Journal of Mining Science and Technology, 24 (2014) 859–864. https://doi.org/10.1016/j.ijmst.2014.05.019

[17] R. E. Delina, J. Paulo H. Perez, V.V. Roddatis, J.A. Stammeier, D. Prieur, A.C. Scheinost, M.M. Tan, J.J.L. Garcia, C.A. Arcilla, L.G. Benning, Immobilization of chromium by iron oxides in nickel–cobalt laterite mine tailings, Environmental Science & Technology, 59 (11) (2025) 5683–5692. https://doi.org/10.1021/acs.est.4c05383

[18] R. K. Valenta, É. Lèbre, C. Antonio, D. M. Franks, V. Jokovic, S. Micklethwaite, A. Parbhakar-Fox, K. Runge, E. Savinova, J. Segura-Salazar, M. Stringer, I. Verster, M. Yahyaei, Decarbonisation to drive dramatic increase in mining waste–Options for reduction, Resources, Conservation and Recycling, 190 (2023) 106859. https://doi.org/10.1016/j.resconrec.2022.106859

[19] M. Tayebi-Khorami, M. Edraki, G. Corder, A. Golev, Re-thinking mining waste through an integrative approach led by circular economy aspirations, Minerals, 9 (5) (2019) 286. https://doi.org/10.3390/min9050286

[20] S. Stanković, S. Stopić, M. Sokić, B. Marković, B. Friedrich, Review of the past, present, and future of the hydrometallurgical production of nickel and cobalt from lateritic ores, Metallurgical and Materials Engineering, 26 (2020) 199–208. https://doi.org/10.30544/513

[21] D. Deniyatno, M. Saranga, Y. Supriyatna, Kinetics study of leaching ore nickel laterite using hydrochloric acid at atmospheric pressure, RISET Geologi dan Pertambangan, 32 (2022) 14–24. https://doi.org/10.14203/risetgeotam2022.v32.1163

[22] Z. Zhao, H. Li, C. Wang, An integrated sulfation-roasting-leaching process for coextraction of nickel and cobalt from laterite ores with enhanced SO_3 recovery, ACS Sustainable Resource Management, 2 (1) (2025) 201–211. https://doi.org/10.1021/acssusresmgt.4c00437

[23] D. Georgiou, V. Papangelakis, Sulphuric acid pressure leaching of a limonitic laterite: Chemistry and kinetics, Hydrometallurgy, 49 (1998) 23–46. https://doi.org/10.1016/S0304-386X(98)00023-1

[24] Y. Li, M. Yang, M. Pentrak, H. He, Y. Arai, Carbonate-enhanced transformation of ferrihydrite to hematite,

Environmental Science & Technology, 54 (21) (2020) 13701–13708. https://doi.org/10.1021/acs.est.0c04043

[25] N. Jenkins, X. Zhou, M. Bhowmick, C. McLeod, M. Krekeler, Investigation into the stability of synthetic goethite after dynamic shock compression, Physics and Chemistry of Minerals, 51 (2024) 12. https://doi.org/10.1007/s00269-024-01279-4

[26] G. Dublet, F. Juillot, G. Morin, E. Fritsch, D. Fandeur, G. E. Brown, Goethite aging explains Ni depletion in upper units of ultramafic lateritic ores from New Caledonia, Geochimica et Cosmochimica Acta, 160 (2015) 1–15. https://doi.org/10.1016/j.gca.2015.03.015

[27] F. He, B. Ma, C. Wang, Y. Zuo, Y. Chen, Dissolution behavior and porous kinetics of limonitic laterite during nitric acid atmospheric leaching, Minerals Engineering, 185 (2022) 107671. https://doi.org/10.1016/j.mineng.2022.107671

[28] G. Kesavan, M. Pichumani, S.-M. Chen, Influence of crystalline, structural, and electrochemical properties of iron vanadate nanostructures on flutamide detection, ACS Applied Nano Materials, 4 (2021) 5883–5894. https://doi.org/10.1021/acsanm.1c00802

[29] K. M. Moya-Canul, F. J. Flores-Ruiz, J. C. Leal-Zayas, R. Silva-González, S. A. Tomás, J. M. Yañez-Limón, Influence of nickel incorporation and thermal treatment under atmospheric conditions and controlled oxygen flow on the ferroelectric and electrical properties of $BiFeO_3$ thin films obtained by sol-gel, Journal of Alloys and Compounds, 1010 (2025) 178015. https://doi.org/10.1016/j.jallcom.2024.178015

[30] X. Gao, Study on the mineral processing technology of copper-nickel sulfide ore, Journal of Engineering and Applied Science, 72 (1) (2025) 29–38. https://doi.org/10.1186/s44147-025-00596-x

[31] R. Chong, Z. Wang, M. Fan, L. Wang, Z. Chang, L. Zhang, Hematite decorated with nanodot-like cobalt (oxy)hydroxides for boosted photoelectrochemical water oxidation, Journal of Colloid and Interface Science, 629 (2023) 217–226. https://doi.org/10.1016/j.jcis.2022.09.024

UTICAJ SADRŽAJA NIKLA I NJEGOVOG OBLIKA POJAVLJIVANJA NA PONAŠANJE LATERITNIH RUDA NIKLA TOKOM LUŽENJA SUMPORNOM KISELINOM POD VISOKIM PRITISKOM

Aad Alief Rasyidi Baking [a, *], Lejun Zhou [a], Wei Liu [b]

[a] Fakultet za metalurgiju i životnu sredinu, Central South University, Čangša, Kina
[b] Sektor za istraživanje i razvoj kompanije QMB Indonesia, Morovali, Indonezija

Apstrakt

U ovom istraživanju procenjen je uticaj sadržaja nikla i njegovog oblika pojavljivanja na ponašanje lateritnih ruda nikla tokom luženja sumpornom kiselinom pod visokim pritiskom (HPAL) na temperaturi od 250 °C. U studiji su korišćene tri vrste ruda: ruda 1 (ultra-niskosadržajni limonit, 0,73 mas.% Ni), ruda 2 (limonit, 1,34 mas.% Ni) i ruda 3 (saprolit, 2,00 mas.% Ni). Mineraloška ispitivanja (XRD, SEM i EPMA) sprovedena su radi dobijanja uvida u faze koje sadrže nikl i u karakteristike matrice rude. Rezultati pokazuju da viši sadržaj nikla ne dovodi nužno do većeg stepena izdvajanja. Ruda 1, iako sa najnižim sadržajem nikla, ostvarila je najveći stepen ekstrakcije Ni (97,25%) i Co (98,49%) u eksperimentalnim uslovima pri odnosu kiseline i rude (A/O) od 0,40. Ovakav visok stepen izdvajanja nikla pripisuje se strukturnoj supstituciji nikla u getitu, oksidu gvožđa koji se lako rastvara u HPAL procesu. Ruda 2 takođe sadrži getit kao dominantnu fazu i postigla je slične stepene izdvajanja Ni (97%) i Co (98%); međutim, pri višim količinama kiseline došlo je do blagog smanjenja izdvajanja kobalta usled njegove koprecipitacije sa hematitom. Ruda 3 posedovala je najveći sadržaj nikla, ali i najnižu efikasnost luženja (<90% Ni). Ovakvo ponašanje pripisuje se činjenici da je nikl vezan i u getitu (lako luživa faza) i u lizarditu (teže luživa faza). Silikatna matrica lizardita i povišen sadržaj magnezijuma ograničili su efikasan opseg kiselosti, čime je smanjena selektivnost izdvajanja nikla tokom HPAL procesa.
Rezultati naglašavaju da je mineraloški oblik pojavljivanja nikla značajniji faktor od samog sadržaja nikla pri određivanju efikasnosti luženja. Stoga limonitne rude sa nižim sadržajem nikla, ali povoljnom mineralogijom, mogu predstavljati perspektivnu sirovinu za ekološki prihvatljivu i održivu hidrometaluršku ekstrakciju nikla.

Ključne reči: *Lateritna ruda nikla; Ponašanje pri luženju; Efikasnost izdvajanja; Limonit; Saprolit*